*Clay Minerals*, (2007) **42**, 415–435

# The petrography of weathering processes: facts and outlooks

A. MEUNIER*, P. SARDINI, J. C. ROBINET AND D. PRÊT

*University of Poitiers, HYDRASA – UMR 6532 INSU-CNRS, 40 avenue du Recteur Pineau 86022 Poitiers Cedex, France*

(*Received 30 March 2007; revised 30 October 2007*)

ABSTRACT: Rock weathering has been investigated from atomic to global scales through the different but complementary approaches of mineralogy, petrography, geomorphology and geochemistry. The sequences of mineral reactions involved in the alteration process are now well known. They explain the global trend of weathering phenomena but do not account for the actual rock transformation dynamics. In particular, they ignore the intimate relation of the mineral reaction progress with the increase in connected porosity. At the hand specimen scale, heterogeneity is the rule: mineral reactions are controlled by local physicochemical conditions. Alteration processes depend largely on the rock microstructure properties. They proceed through nearly-closed, semi- and completely open microsystems which are interconnected by fractures or pores. Before being leached out by the solutions which flow in the large fractures (flux), the soluble elements migrate inside the connected porosity through chemical diffusion. The dissolution of the primary minerals is mediated through local gradients of chemical potential. With increasing alteration, the rock porosity increases, as does the length of the fluid passageways and their constrictivity and tortuosity. Consequently, the apparent diffusion coefficient for the most soluble elements decreases. The amplitude of the chemical potential gradients for the most soluble elements is reduced by the progressive coating of the reactive surfaces by clays and Fe oxyhydroxides. The residence time of these elements inside the weathered rock increases as alteration progresses; an effect enhanced by their temporary adsorption on the exchangeable sites of clays and Fe oxyhydroxides. Consequently, the weathering rate decreases with time. A possible new way to calculate weathering rates could be to measure the residence time of soluble elements inside the different microsystems during their migration towards the diluted solution which occurs in the large fractures.

KEYWORDS: weathering, diffusion, microsystems, mass balance, residence time.

Weathering became a subject for research as soon as the chemical analysis of silicates was made possible at the beginning of the 19th century. One of the earliest pioneering works was published by Ebelmen (1847), who gave the first mass-balance calculation of weathered rocks (sandstones, basalts). Since then, many other studies have been published especially during the last four decades. This important literature (reduced here to some representative papers) can be divided into six classes according to the specific weathering domain under concern: (1) the mineral reaction mechanisms from atomic to macro scales (Meunier, 1980; Eggleton & Buseck, 1980; Eggleton, 1984; Banfield & Eggleton, 1988, 1990); (2) the relationship between alteration processes and landscape geomorphology (Millot, 1964; Ollier & Pain, 1996); (3) the experimental alteration of rocks and minerals (Berner & Schott, 1982); (4) the thermodynamics of solutions (Garrels & Christ, 1965; Tardy, 1993); (5) the chemical mass balance at different scales (profile, watershed, continent) using major and

* E-mail: alain.meunier@univ-poitiers.fr
DOI: 10.1180/claymin.2007.042.4.01

minor elements or stable isotopes (Allègre *et al*., 1986; Gaillardet *et al*., 1999); and (6) the alteration rates (Colman, 1986; Dethier, 1986; Whitehouse *et al*., 1986; White & Brantley, 1995; Sak *et al*., 2004).

Because the six study domains are based on different methods and address different analytical scales from atomic to continental, their respective results are difficult to integrate. This leads to large differences in calculated weathering rates (White & Brantley, 2003). However, even if still unknown, a strong link must exist between the different scales. Indeed, any chemical balance calculated at the scale of an alteration profile represents the summation of the effects of all the mineral reactions which occur at the microsystem scale. In the same way, any calculation of weathering rate averages the dissolution-precipitation rates experienced by the primary and secondary minerals during the alteration process.

Because the weathering rate is a fundamental parameter in the evolution of the Earth's surface, there has been significant effort over the last decade to improve methods of calculation and analysis. However, the reliability of such techniques is questionable since two obstacles were not overcome until recently (White & Brantley, 2003): (1) the alteration rates measured through experimentation are always several orders of magnitude greater than those measured in natural conditions; and (2) in natural conditions, the weathering rate decreases with time.

These two obstacles originate from the difficulty in taking into account the way mineral reactions actually proceed in a given rock, as well as the fact that the evolution of primary and secondary mineral distributions and porosities in particular, have been outside our analytical capabilities until recently.

The goal of this paper is to discuss the methods that have been employed to calculate weathering rates and to present the potential of quantitative petrology to overcome the two obstacles outlined by White & Brantley (2003).

## THE MECHANISM OF WEATHERING

### *The two concepts of rock weathering: sequences of alteration minerals vs. microsystems*

The fate of any rock at the Earth's surface, irrespective of origin or composition, is to reduce its chemical disequilibrium with respect to meteoric water which constantly flows within it. To do this, rocks tend to transform into a chemically homogeneous fine-grained material which approaches equilibrium with the surrounding solutions. To gain homogeneity, a rock must undergo physical, chemical and mineralogical transformations by: (1) reduction of the average crystal size by fragmentation of primary minerals and crystallization of clay minerals which are always small (Meunier, 2006); and (2) reduction of the number of mineral species as alteration continuously impoverishes the rock composition. The general trend is towards an ideal monomineralic composition which reduces the inter-crystalline chemical differences.

The progression towards the ultimate monomineralic stage is classically described as a four-step reaction sequence. The first step is the formation of secondary phyllosilicates where the chemical composition is close to that of the parent minerals. These form through nucleation and crystal growth processes if their parent minerals are not phyllosilicates. If they are, the secondary phyllosilicates partially inherit the primary phyllosilicate structure. Such a process has been suggested for the alteration of biotite, muscovite and chlorite crystals (see Wilson, 2004). The second step is the recrystallization of all the secondary phyllosilicates into more dioctahedral versions through the oxidation of $Fe^{2+}$ ions and the loss of bivalent cations ($Mg^{2+}$, $Ni^{2+}$ or $Mn^{2+}$). Most often, during this process, some of the $Fe^{2+}$ ions are expelled from the crystal lattices of the silicates and precipitate in the $Fe^{3+}$ state, forming oxyhydroxide minerals. The third step is the formation of an homogeneous rock composed of kaolinite/halloysite + Fe-Mn oxyhydroxides; a process which occurs irrespective of the parent rock composition. The fourth step is the total dissolution of the silicates leading to bauxite or duricrust rocks which are essentially composed of Al and Fe oxyhydroxides.

If the alteration sequence concept successfully depicts the progress of alteration at a large scale, with each of the steps being predominant over a range of climatic-topographic conditions, it is not necessarily perfectly applicable at the scale of altered rock facies (saprock, saprolite) or soil, e.g. biotite alteration is classically described as a four-step sequence (Wilson, 2004): (0) biotite → (1) tri-vermiculite → (2) di-vermiculite ± kaolinite → (3) kaolinite + Fe oxyhydroxides → (4) gibbsite + goethite. Each step of the alteration sequence

characterizes the major climatic areas from boreal to tropical conditions. However, despite the apparently logical relationship with increasing alteration degree, it does not adequately describe how biotite weathers in a granite for two reasons: (1) the alteration of biotite crystals does not begin systematically by step 1; and (2) different secondary mineral assemblages (steps) are concomitantly formed from biotites at the thin-section scale. Therefore, taking into account this information, it is necessary to investigate the weathering mechanisms in terms of microsystems. This concept was first presented by Korzhinskii (1959) to explain the local-scale equilibria in metasomatized rocks and has since been applied to the analysis of mineral reactions in weathered granites (Meunier & Velde, 1979). A microsystem is located at each water-parent mineral contact and is composed of the primary and secondary minerals and local solutions. Innumerable microsystems exist in a single petrographical thin section. However, they belong to only a few categories: closed, semi-open and completely open. The greater the number of microsystem categories, the greater the rock heterogeneity. Highly altered rocks such as duricrusts in lateritic profiles are characterized by only one type of microsystem in which Al and Fe oxyhydroxides form.

Consider, for example, the alteration of biotite crystals in weakly weathered granitic rocks, where three types of microsystems are observable at the thin-section scale (numbers refer to drawings in Fig. 1):

(1) *Biotite-orthoclase and biotite-plagioclase contacts*: illite crystallizes inside the K-feldspar along the intergranular joint with biotite (Fig. 1a) or biotite is destabilized into a trioctahedral vermiculite + kaolinite assemblage along the open intergranular join with the plagioclase crystal (Fig. 1b).

(2) *Internal destabilization of a biotite crystal*: biotite is replaced by a trioctahedral vermiculite + kaolinite + Fe oxyhydroxides assemblage.

(3) *Microfissure inside a biotite crystal*: kaolinite + Fe or Ti oxyhydroxides are formed directly from the biotite along the microfracture (Fig. 1).

It is obvious that weathering cannot simply be reduced to a set of mineral reaction sequences. Indeed, any altered rock not only changes on a mineral-composition basis but is also modified texturally (porosity, permeability, surface type and area of unstable minerals exposed to solutions etc.). The microsystem concept integrates the chemical, mineralogical and physical parameters because it is based on petrographical analyses. It helps us understand how rocks are transformed in supergene conditions at the hand-specimen scale.

## *A qualitative model for rock weathering*

Figure 1 shows a simplified representation of the microsystem-porosity relationships for a weakly altered granite. It can be used as a basis for qualitative modelling of weathering processes in which connected voids belong to three categories (Fig. 2): (1) primary porosity ($\Phi_1$) and microfracture dead ends (resident fluids); (2) microfractures (capillary fluid); and (3) large fractures (gravity flowing fluids).

As soon as water infiltrates the unweathered rocks (time $t_0$), a set of different microsystems is activated along the fluid pathways (connected microfractures). The total length ($l$) of the diffusion path integrates all the pathways connecting the pores with the microfractures. Near-equilibrium conditions are established in narrow pores or dead-end microfractures (microsystem 3 in Fig. 2) where the fluids are resident. In these regions the alteration rate is controlled by surface processes (dissolution of primary and growth of secondary minerals) rather than chemical diffusion. The mineral reactions are nearly isochemical since only small amounts of alkalis and silica are lost. Hence these microsystems are almost entirely closed. Conversely, far-from-equilibrium conditions prevail in the vicinity of large water passageways (microsystem 1 in Fig. 2), as the solutions are constantly diluted by meteoric water inputs (completely-open microsystem). Consequently, for a given ion species ($i$), the concentration varies from high ($C_{i,\mathrm{eq}}$) to low ($C_{i,\mathrm{min}}$) values in the nearly-closed to completely-open microsystems, respectively. The difference in concentration ($C_{i,\mathrm{eq}} - C_{i,\mathrm{min}}$) creates a difference in chemical potential which varies between the largest ($\mu_{i,\mathrm{near}}$) and smallest ($\mu_{i,\mathrm{far}}$) values with distance to the large fractures. This establishes a chemical potential gradient ($d\mu_i/dl$) between the nearly-closed and the completely-open microsystems. This gradient is a continuous function whose limits are given by $C_{i,\mathrm{eq}}$ and $C_{i,\mathrm{min}}$; the near- and far-from equilibrium concentrations, respectively.

The gradient may be steep or gentle depending on the length of the diffusion path. However,

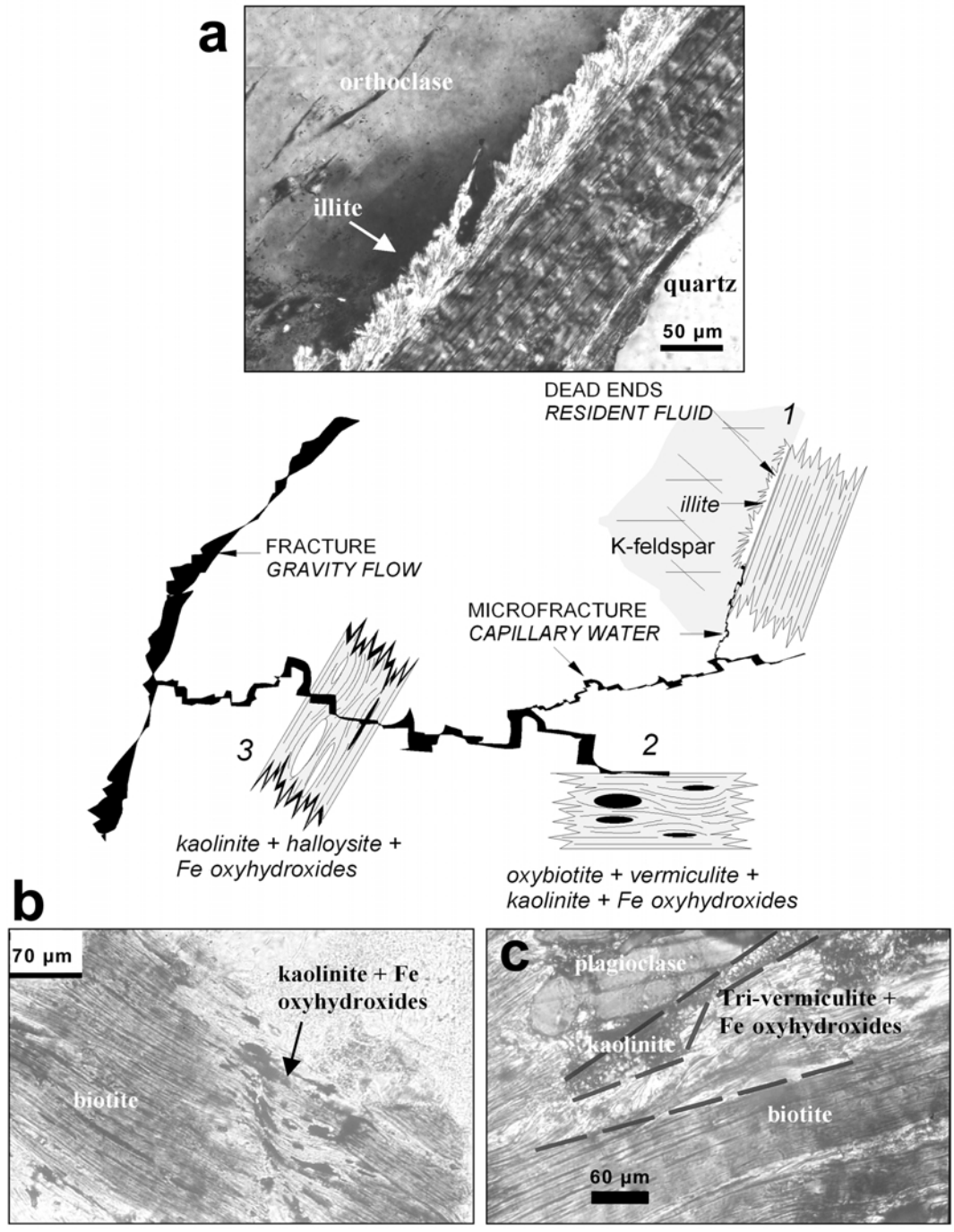


FIG. 1. Example of biotite microsystems in a weakly altered granite (La Rayrie, Deux Sèvres, France). (a) Contact microsystem at the intergranular joint showing the growth of illite crystals inside K-feldspar. (b) Biotite and plagioclase concomitantly altered along their intercrystalline joint. (c) Alteration of a biotite crystal into kaolinite + Fe oxyhydroxides along a microfracture.

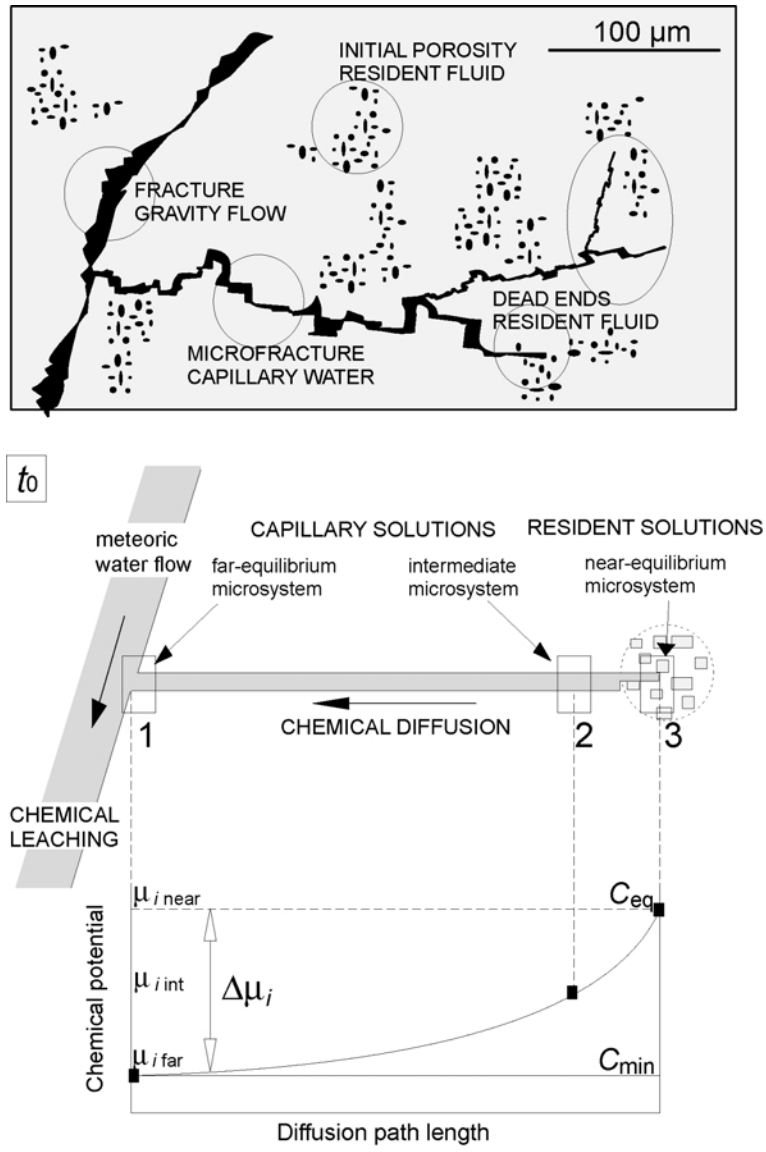


FIG. 2. Simplified theoretical model representing the petrographical relations between different microsystems and the variation of the chemical potential of a given element $i$ ($\Delta\mu_i$) at the beginning of the alteration processes (time $t_0$). The $\Delta\mu_i$ varies between two end-member chemical potentials established in near ($\mu_{i\ near}$) and far ($\mu_{i\ far}$) equilibrium conditions, respectively, for concentrations in equilibrium with the dissolving mineral ($C_{i\ eq}$) and the water passageways ($C_{i\ min}$). Secondary phases are considered to precipitate at intermediate chemical potential ($\mu_{i\ int}$) conditions.

irrespective of angle, the gradient curve intersects the formation conditions for different secondary products in near-, intermediate- ($\mu_{i,int}$) or far-from-equilibrium microsystems. For instance, K-feldspar alteration gives illite, smectite + kaolinite or kaolinite in near-, intermediate- and far-from-equilibrium microsystems, respectively. In tropical regions, the far-from-equilibrium conditions are encountered in gibbsite-forming microsystems. The limit for the far-from-equilibrium conditions is given by the congruent dissolution of feldspar. These extreme conditions are frequently used in

experiments for the measurement of dissolution rates.

### *The progression of alteration*

Dissolution of the primary mineral in a rock creates new voids which may be completely empty or partially filled by newly formed clay minerals, oxyhydroxides or amorphous material. The resulting fine-grained matter is assigned as primary plasma (Bisdom, 1967). The secondary porosity ($\Phi_{II}$) is given by:

$$\Phi_{II} = (V_v - V_m)/V_r \times 100 \quad (1)$$

where $V_v$, $V_m$ and $V_r$ are the volumes of the dissolution voids, secondary minerals and rock, respectively. Regardless of the quantities of the newly formed phases, the secondary porosity increases globally because the alteration products never completely replace the dissolved volume, even in the case of pseudomorphic replacement of the primary crystals (Putnis, 2002). Figure 3 schematically demonstrates the integration and contribution of all the microsystems which are active from $t_0$ to $t_1$.

As the rock porosity ($\Phi_I + \Phi_{II}$) increases, the geometrical parameters of the connected pathways change (Sardini *et al*., 2001; Sausse *et al*., 2001). The solutions increasingly invade the rock as alteration progresses, causing the fluid passageways (microfractures and pores) to widen continuously as dissolution is enhanced by the chemical potential difference. Hence, the fluids which were originally stagnant in a given place (resident fluid) begin to move (capillary) after the alteration reactions have occurred because the passageways have been enlarged. This changes the local chemical conditions leading to new chemical and mineral reactions. As a result the secondary minerals formed at $t_1$ are no longer stable.

With increasing time ($t_x$), the alteration progresses towards the unweathered zones of the rock. New dissolution voids are formed while new secondary phases crystallize (Fig. 4). Concomitantly, the local physicochemical conditions imposed in the previously altered zones evolve. (1) Primary minerals are dissolved into solution causing porosity to increase, leading to the continuous geometrical evolution of the diffusion paths as they become increasingly branched and extensive. This results in the increase of the average length of diffusion pathways globally. (2) The major passageways in which the solutions have the lowest chemical concentrations are progressively coated by clay mineral + Fe oxyhydroxide deposits. In other words, the fluids are 'insulated' from the parent rock by a new composite rock whose reactive surface is formed of clay minerals + Fe oxyhydroxides and any residual primary crystals. The coatings globally reduce the dissolution rate of the primary mineral (Nugent *et al*., 1998; Hodson, 2003; Ganor *et al*., 2005). They also reduce the rate of chemical diffusion between the fractures and the microporous matrix (diffusion matrix).

Mostly, the large passageways are coated by monophase silicate assemblages, i.e. kaolinite, Fe-beidellite or nontronite in granite, gabbro or lherzolite respectively (Meunier & Velde, 1979; Ildefonse, 1980; Fontanaud & Meunier, 1983), solutions which are rapidly renewed in these passageways are in equilibrium with these phases. The chemical equilibrium between the solutions and the clay deposits (cutan) represents the new far-from-equilibrium conditions imposed on the system at time $t_x$. The difference in chemical potential for most of the diffusion path is reduced to the $\mu_{int} - \mu_{cut}$ value. Consequently, the chemical potential gradient decreases for two reasons: (1) the increase in the diffusion path length (arrow a in Fig. 4); and (2) the decrease in potential difference (arrow b in Fig. 4).

### *The evolution of the system towards homogenization*

Irrespective of parent rock-type, the most altered zones (saprolite) in weathering profiles are fine-grained microporous materials. The initial rock microstructure disappears completely by collapsing or sliding under gravity. The unaltered remnants are fragmented and dispersed throughout a clay-rich matrix forming the secondary plasma (Meunier & Velde, 1979). The clayey matrix is itself a fine-grained mixture of tiny parent crystal debris and clays which were previously formed inside primary plasma microsystems. Because the chemical compositions of the clay matrix and the cutans are very similar, the difference in chemical potential between the large connected pores and the microporous matrix is reduced compared to that of the saprock (Fig. 5). Concomitantly, the parent rock remnants and the large primary crystal debris continue to be altered inside residual microsystems which still produce a primary plasma.

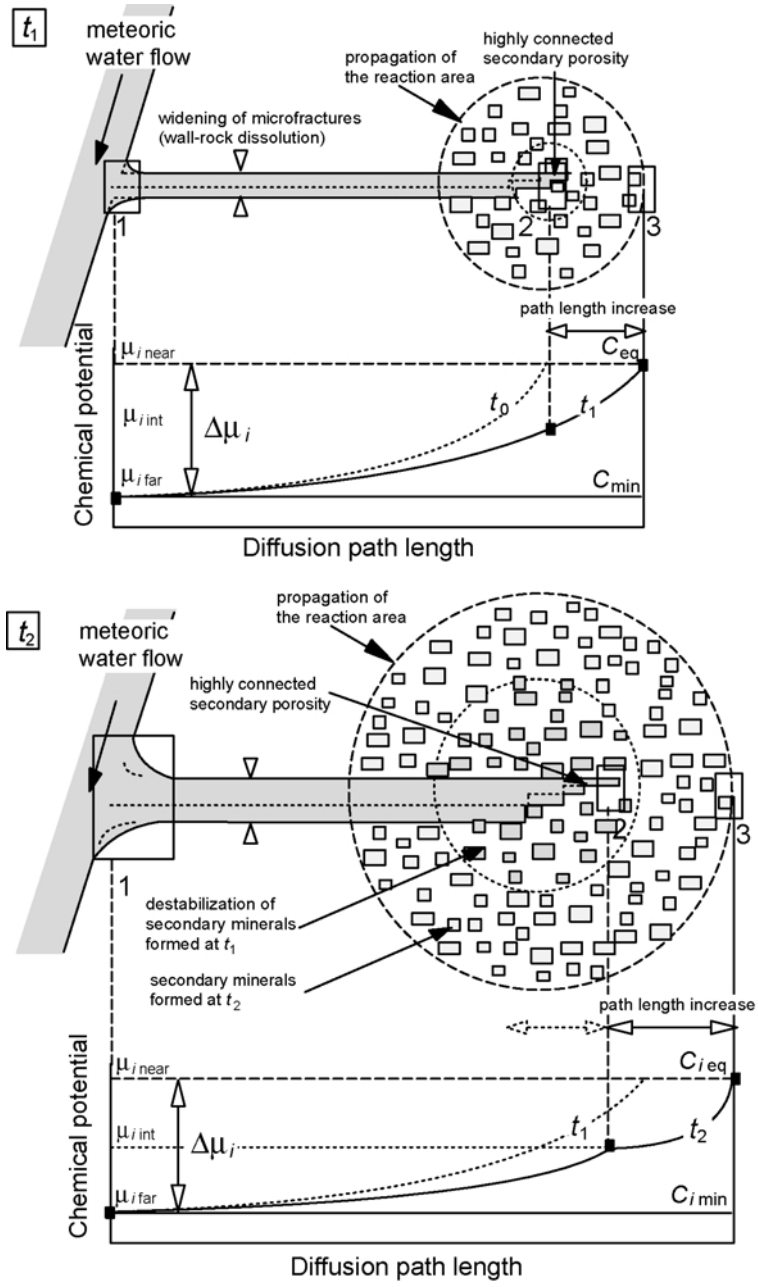


FIG. 3. Simplified model for the evolution of the rock properties with increasing alteration from $t_1$ to $t_2$. The chemical potential difference changes due to the formation of a secondary porosity which is increasingly connected, causing the lengths of the diffusion paths to increase. The limits of the difference are always the end-member chemical potentials established in near- and far-equilibrium conditions ($\mu_{i\ near}$ and $\mu_{i\ far}$).

To summarize, during weathering processes, several reactions concomitantly transform each primary mineral of a given rock according to the different properties of individual microsystems. For example, gibbsite is not automatically the ultimate weathering product of granitic rocks. It may also

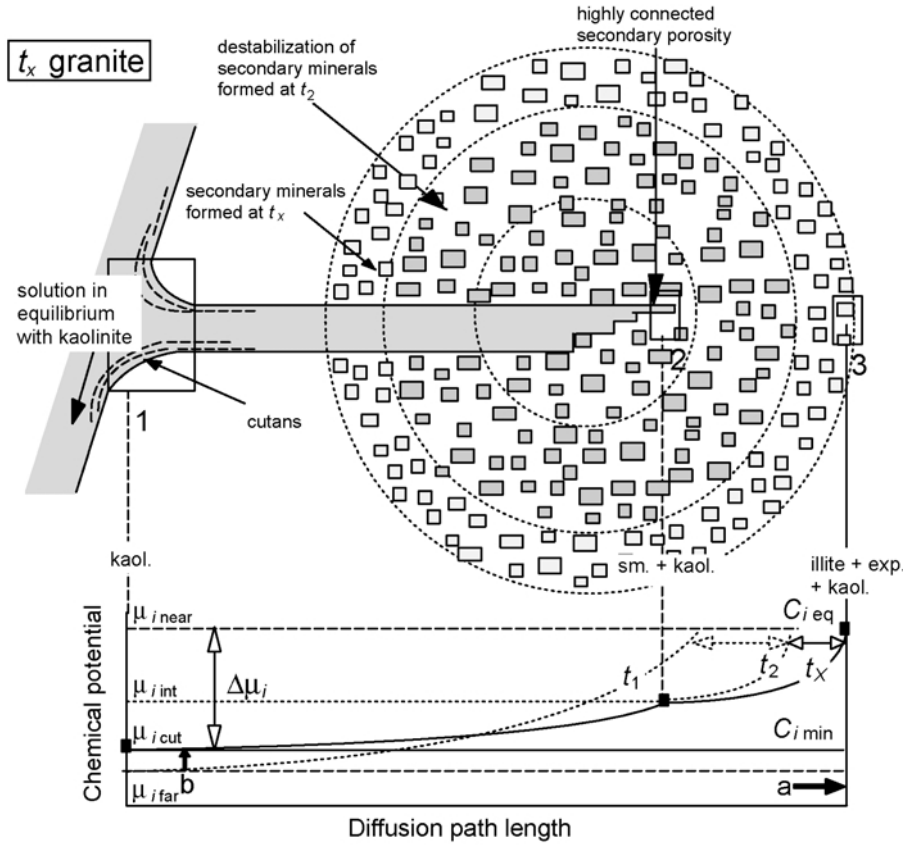


FIG. 4. State of the weathering system at $t_x$ for a granite rock. The length of the diffusion paths is continuously increasing (arrow a). The difference in chemical potential ($\Delta\mu_i$) is reduced by the equilibration of meteoric waters with the clay species forming the cutans (arrow b). An increasing amoumt of the diffusion path experiences a reduced potential difference ($\mu_{int}-\mu_{cut}$).

crystallize directly in the saprock of a weathered profile developed under temperate climates if formed in specific topographic conditions such as steep mountain slopes which favour intense leaching. During weathering, a rock experiences a multi-equilibrium state through numerous types of micro-system, with each imposing specific chemical conditions according to local chemical differences. Although saprock remnants still persist in the saprolites, indicating some residual microsystems may be temporarily active, increasing alteration leads to a progressive reduction in the number of different microsystem types. After long periods of weathering, only one type of microsystem remains active. The ultimate alteration stage leads to the formation of ferricrete or bauxites which are fine-grained, nearly monomineralic new rocks. At this point the homogenization process is complete (Fig. 6).

## CALCULATION OF THE WEATHERING RATE

### *Calculating mass balance and weathering rate*

The addition or subtraction of chemical components is calculated by comparing altered and unaltered samples. This assessment is related to an invariant parameter which can be physical (volume) or chemical (inert component amount). It is important to consider that the samples used in this study are of hand-specimen scale. As a result, petrographical evidence of volume preservation or chemical evidence of residual concentrations of a perfectly inert component are not as easy to establish. White *et al.* (2001) used a set of inert components (Ti, Zr and Nb) to calculate the volume changes. Considering one of the inert conservative chemical species (*i*), the volume change is given by:

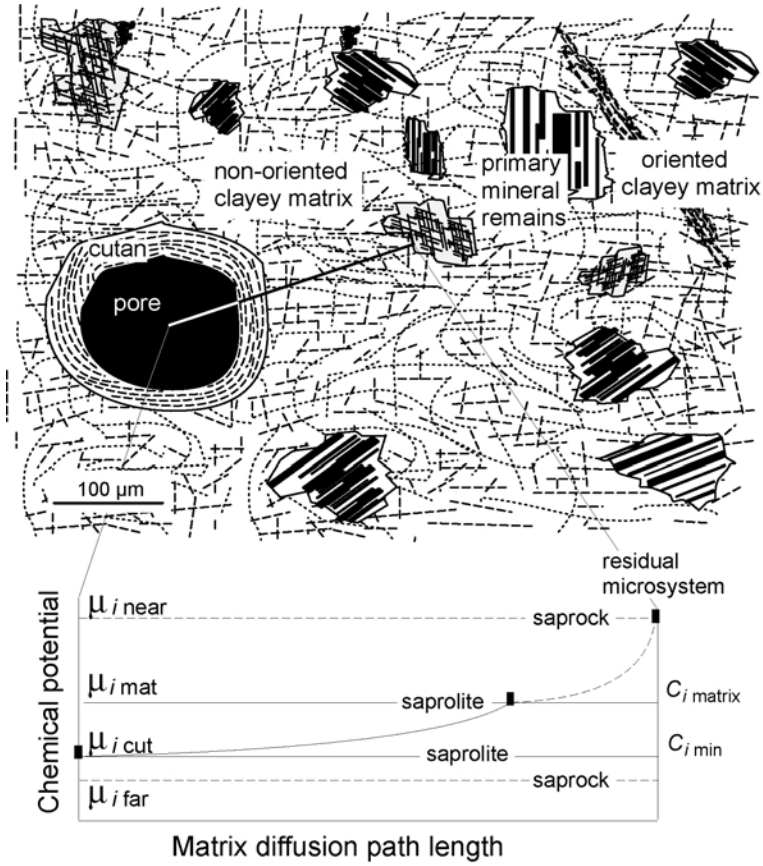


FIG. 5. Schematic representation of the relationship between the saprolite microstructure and the differences in chemical potential between the solution passageways (pores) and the clayey matrix. The parent rock (or primary crystal remains) form residual microsystems in which the secondary phases are similar to that formed in the saprock.

$$\varepsilon_i = \frac{\rho_p C_{i,p}}{\rho_w C_{i,w}} - 1 \qquad (2)$$

where $\rho_p$ and $\rho_w$ are the densities (g cm$^{-3}$) of the protolith and weathered samples, respectively, and $C_{i,p}$ and $C_{i,w}$ are the concentrations (mol g$^{-1}$) of species $i$ in the protolith and weathered samples, respectively.

If $\varepsilon_i$ is equal to zero, the weathering process is volume conservative. If $\varepsilon_i$ is greater or less than zero, weathering will lead to the expansion or contraction of the rock structure, respectively. White *et al*. (2001) showed that granite alteration is almost entirely isovolumetric (saprock) except in limited zones where the structure is compressed (saprolite).

Using mass-balance calculations for the Panola granite profile, White *et al*. (2001) showed that weathering proceeded through four successive alteration stages. From stage 1 to stage 4, the progress of the weathering reactions is controlled by a continuous increase in the hydraulic conductivity. The authors successfully demonstrated that the plagioclase and K-feldspar relative weathering rates vary in the different rock facies of the profile (Table 1). These results are encouraging and imply that it may be possible to determine a global weathering rate for the Panola granite. However, discrepancies in the published alteration rates of minerals in experimental and natural conditions make it necessary to reconsider the weathering processes themselves.

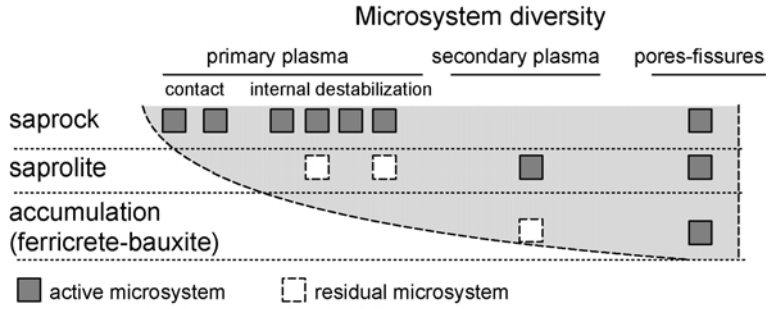


FIG. 6. Schematic representation of the homogenization process through the reduction of the number of different microsystem types. The initial number of microsystems in the saprock depends on the mineralogical composition and the microstructure of the parent rock. Residual saprock microsystems may locally and temporarily survive in the saprolite. Plasma is a fine-grained material formed in the altered zones of minerals from texture-conservative saprock (primary plasma) or texturally modified saprolite (secondary plasma).

### *Deciding the optimal parameter for the measurement of alteration progress*

Weathering reactions can be regarded simply as coupled dissolution and crystallization processes. The dissolution creates new voids (secondary porosity) while crystallization creates new solids. The first process decreases rock density while the second one increases it, i.e. the apparent density is a function of the dissolution and crystallization rates. When measured in volume-conservative altered zones (weathered bedrock and saprock), the apparent density of weathered samples integrates the effects of the two processes. Consequently, the apparent density varies with the difference between the dissolution and the crystallization rates. Both rates depend on the local chemical conditions which change spatially in the weathering profile. Such variations in alteration intensity can be shown by the difference in the apparent density between unaltered and altered samples ($\Delta_{appdens}$):

$$\Delta_{appdens} = \left( \frac{(density_{unweathered} - density_{weathered})}{density_{weathered}} \right) \times 100 \quad (3)$$

When applied to the Panola weathered profile studied by White *et al*. (2001), the $\Delta_{appdens}$ variation reaches 30% in the weathered bedrock at the bottom of the profile and decreases to ~25% in the saprock (Fig. 7a).

Transitory equilibria between the fluid and the secondary phases are established in the different microsystems scattered along the diffusion paths. The dissolution of the primary minerals does not stop until the chemical potential difference is reduced to zero. Hence, the dissolution voids widen continuously or form in the unstable primary minerals, but at a decreasing rate. The variation in density caused by the dissolution voids ($\Delta_{dissoldens}$) is important during the early alteration

TABLE 1. Summary of the four alteration-stage characteristics of the Panola granite weathering profile (from White *et al*., 2001).

| Stage | Rock facies | Permeability | Dissolution rate control | |
|---|---|---|---|---|
| | | | K-feldspar | Plagioclase |
| 1 | Pristine granite | Low primary, no secondary | Unweathered | Unweathered |
| 2 | Weathered bedrock | Low primary + low secondary | Fluid transport | Fluid transport |
| 3 | Saprolite | Moderate permeability | Fluid transport | Kinetics |
| 4 | Soil | High permeability | Kinetics | Kinetics |

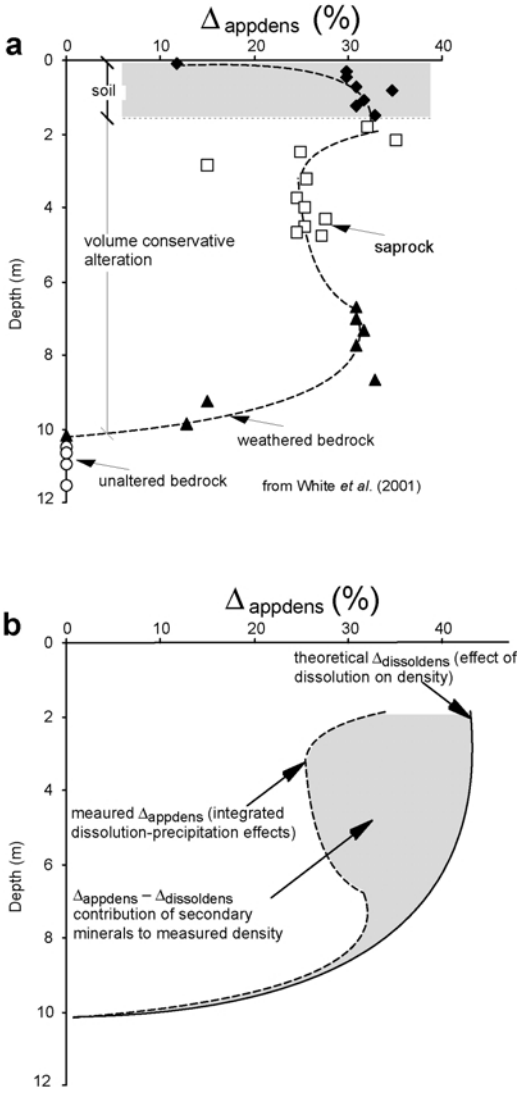


FIG. 7. Variation of the $\Delta_{appdens}$ (see equation 3) with depth in a weathering profile of the Panola granodiorite (data from White *et al*., 2001). (a) Measured variation (the major altered zones in the profile are indicated by different symbols). A simplified variation curve is given by the dashed line. (b) Theoretical interpretation of the respective effects of increasing volumes of dissolution voids (full line) and secondary phases (grey zone) on $\Delta_{appdens}$.

stage (altered bedrock) but decreases in the saprock stage. The theoretical $\Delta_{dissoldens}$ and measured $\Delta_{appdens}$ curves are represented by the full and dashed lines, respectively, in Fig. 7b. The difference (grey area) is due to the formation of secondary minerals which partly compensate for the removal of primary material and the decrease in rock density. To summarize, the volume of the secondary voids or dissolution voids ($V_d$) can be used as a criterion for reaction progress because dissolution occurs continuously, even if its rate decreases with time. Hence, the mass of the dissolved components ($M_d$) is a function of $V_d$:

$$M_d = f(V_d) \quad (4)$$

With the discovery of this relationship, the problem became the accurate and reliable measurement of the dissolution void volume ($V_d$), necessary for the calculation. Gas adsorption methods were shown to be inappropriate because N or Ar atoms are adsorbed on any free surfaces including those of the secondary products (Brantley & Mellott, 2000). The geometrical porosity measurement methods based on SEM observations, recommended by White & Brantley (2003), are convenient at small scales but difficult to extrapolate to larger fields. Indeed, the practical scale of SEM volume investigations for minerals and rocks is on the order of $\mu m^3$–$mm^3$; any extrapolation to volumes several orders of magnitude greater gives questionable results. This drawback is avoided if SEM observations are related to image analysis of autoradiographs obtained from samples impregnated with $^{14}$C-doped polymethylmethacrylate resin ($^{14}$C-PMMA) (Hellmuth *et al*., 1993; Sardini *et al*., 2006). All the connected voids are impregnated even if secondary products are present. This method provides 2D images of the connected porosity with a resolution of a few tens of micrometres from samples several cubic centimetres in size (Fig. 8). To be impregnated, the voids must be connected to the outer surface of the sample and accessible to the MMA monomer. Deuteric pores in feldspar were shown to be inaccessible because of the extreme constriction of their connection pathways: hence, they were measured using SEM observations (Sardini *et al*., 2006). This results in the impregnation method underestimating the total porosity of the unweathered samples.

In the autoradiographs (Fig. 8), the porosity highlighted by the impregnated $^{14}$C-PMMA is illustrated by black and grey areas which correspond to voids and the microporous clayey matrix, respectively. For a unit surface of the studied sample, the porosity in a 2D space is proportional

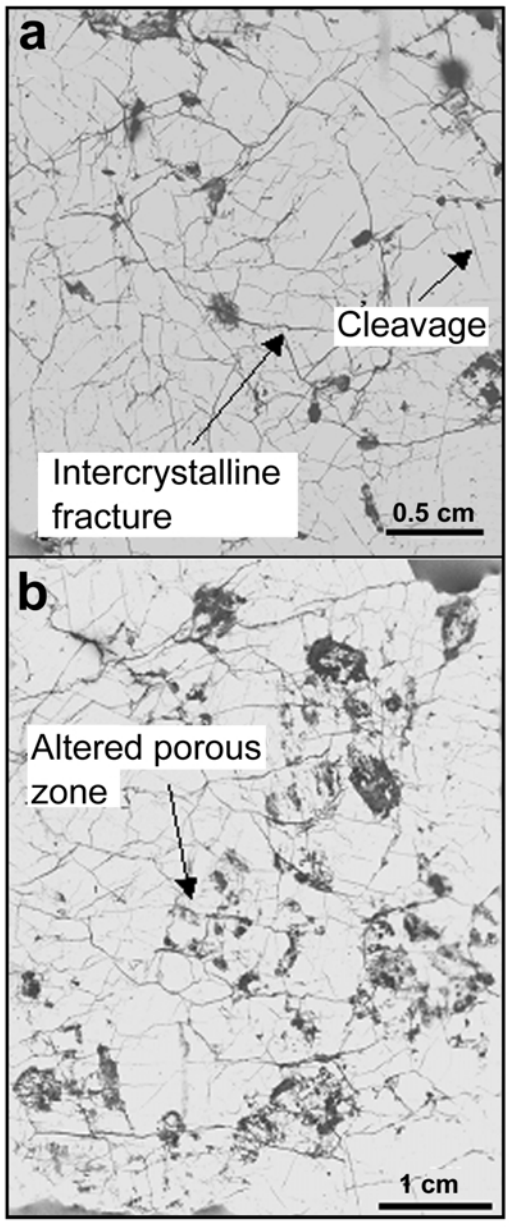


FIG. 8. Autoradiographs of (a) unaltered and (b) altered Palmottu granite samples impregnated with a $^{14}$C-PMMA resin (from Siitari-Kauppi *et al*., 2003). The connected microfractures and cleavages appear as black lines. Zones of diffuse porosity appear as grey areas.

to the summation of the black and grey area ($A$). The effect of dissolution is proportional to the difference between the $A$ values of altered and unaltered samples ($A_{\text{altered}} - A_{\text{unaltered}}$). Using statistics, it is possible to extrapolate the 2D analysis to 3D space and calculate $V_{\text{d}}$. For a given mineral of density ($\rho_x$), the dissolved mass ($M_{dx}$) for each primary mineral species is given by:

$$M_{dx} = V_{dx} \times \rho_x \quad (5)$$

The size and number of dissolution voids (porosity distribution) for each primary mineral in a granite are obtained using the image analysis of a combined map, which is obtained by the superimposition of a mineral map (acid etching–staining methods) with autoradiographs (Oila *et al*., 2005; Sardini *et al*., 2006). The volume of the dissolution voids for a primary mineral ($V_{dx}$) is then measured by integration of the distribution curve. The variation of $V_{dx}$ for each mineral species is determined over the range of fresh to heavily altered samples. Hence, the quantity of dissolved primary minerals ($M_{dx}$) is known for each level of a weathering profile. Once $M_{dx}$ has been found, it is easy to calculate the number of dissolved moles of the parent mineral under concern (e.g. number of moles of oligoclase; $M_{d\text{olig}}$). The number of moles of a particular solute element is then given by stoichiometry (number of moles of solute Na: $M_{d\text{Na}}$).

## WHY DOES ALTERATION RATE DECREASE WITH TIME?

The real question here is how much time is needed for a weathered rock to lose a given mass of a solute element (e.g. $M_{d\text{Na}}$)? Two processes are activated during weathering: (1) the dissolution of the parent crystals; and (2) the transport of the resulting solute out of the rock. The weathering rate is essentially controlled by the slowest process (Brantley, 2005). According to Berner (1978, 1981) and Velbel (1993), the alteration rate is controlled by dissolution and particularly by the solid-fluid interface exchanges. However, taking into account the extreme tortuosity of these interfaces, Hochella & Banfield (1995) claimed that the rate of solution transport in the early alteration stage is zero. Consequently, the migration of solute elements depends only on concentration gradients. This is certainly the best approach to understanding the rock weathering process since it implicitly takes into account the rock microstructure.

### *Reactive mineral surfaces: the roughness parameter*

White & Brantley (2003) showed that the silicate mineral dissolution rates decrease with increasing alteration period, both in experimental and natural conditions. However, even the smallest values obtained in the experiments are several orders of magnitude faster than that calculated for weathering. This led White & Brantley (2003) to introduce a roughness parameter ($\lambda$) in order to reconcile the dissolution rates measured through experiments with those estimated in natural conditions. The surface roughness is defined as the ratio of the Brunnauer-Ennet-Teller (BET) specific surface area to the geometric surface area. It increases with time due to the progressive increase in surface pitting and internal porosity. Using a log-log plot, White & Brantley (2003) considered that $\lambda$ increases linearly with time. Despite the poor correlation (see figure 4, page 491 of White and Brantley, 2003), it has been used to calculate a normalized BET specific surface area equivalent, which is then introduced into the rate equation. This led to a power function which describes the decrease in the weathering rate of the Panola granite with time: $R = 3.1 \times 10^{-13}\ t^{-0.61}$ (mol $m^{-2}$ $s^{-1}$).

White & Brantley (2003) explain that the time-dependency of silicate weathering increases with the duration of weathering. This is due to the increase of the normalized surface area, which was shown to account for a third of the exponential decrease in the weathering rate. However, the results of these studies contain large uncertainties because several parameters are not taken into account. The BET method does not distinguish the surfaces of the dissolving minerals from that of their secondary products (Brantley & Mellott, 2000) and consequently the roughness factor is overestimated. The difficulty in measuring the dissolution surface area for each primary mineral in a weathered rock leads to the reconsideration of what are 'reactive' surfaces. White & Brantley (2003) argued that the dissolution rate decreases with time because the energetically reactive surfaces are depleted by the elimination of the most defective areas and most soluble zones in the minerals. Additionally, the development of leached layers and mineral or organic coatings reduces the diffusion rate of solute elements (Banfield & Barker, 1994; Nugent *et al*., 1998). Gautier *et al*. (2001) showed that the reactive surfaces cannot be directly measured. For experimentally altered quartz, the majority of the surface area measured using the BET method was unreactive etch-pit walls. The dissolution rate does not increase proportionally with etch-pit development, which means that the major effect of etch-pit development is not chemical but physical because it changes the transport parameters.

Pacheco & Alencoão (2006) state that the gap between laboratory and field weathering rates decreases when the rates are normalized to fracture area, which is calculated through the measured hydraulic conductivity and the effective porosity of the rocks. It is remarkable that the decrease in weathering rate according to a power function can be researched at both the atomic (dissolution surface of the minerals) and macroscopic (structure of rock bodies) scales.

### *The theoretical basis of a quantitative weathering model*

The solute flux controlled by chemical diffusion is quantified by a basic Ficks type equation such as that proposed by Hochella & Banfield (1995):

$$J_i = \frac{di}{dt} = \frac{\beta c_i T (C_{i,\mathrm{j}} - C_{i,\mathrm{e}}) A}{\eta l} \qquad (6)$$

where $di/dt$ represents flux ($J_i$) of species $i$ per time $t$ (quantity per unit time, mol $s^{-1}$). By definition a flux is normalized to a unit surface area. It is expressed in mol $s^{-1}$ $m^{-2}$ (this method leads to the removal of the $A$ factor from the right side of equation 1); $\beta$: the geometric constant taking into account the porosity or tortuosity (adimensional); $c_i$: constant that scales the radius of species $q$ (to be coherent with the Stokes-Einstein equation, $c_i$ has to be equal to $k_B/6\pi r$ where $k_B$ is the Boltzman constant and $r$ the radius of the particle); $T$: absolute temperature (K); $C_{i,\mathrm{i}}$ and $C_{i,\mathrm{e}}$: concentration of species $i$ in the internal and external areas of the system, respectively (mol $l^{-1}$); $A$: effective pore area ($m^2$); $\eta$: water viscosity (Pa s); $l$: average length of diffusion paths (m).

Equation 6 is based on the following simplifying assumption: at the top-most surface of dissolving minerals, the effect of the electrical double layer which can be modelled by the increase of water viscosity is ignored. Moreover, this simplification does not take into account the complex ion-solute

interactions which occur in the double layer (Revil, 1999). However, at the hand-specimen scale, the increase of water viscosity with decreasing pore size is negligible in weathered rocks where pores and fractures are usually large (μm–mm).

Several terms of equation 6 can be considered as being approximately constant in weathering conditions. This is the case for temperature at a given latitude, even if it can change with time as argued by White *et al*. (2001). This is also the case for the ($C_{i,\mathrm{i}}-C_{i,\mathrm{e}}$) parameter which is assumed to represent the difference between the concentration of species $i$ at equilibrium with the dissolving mineral ($C_{\mathrm{eq}}$) and that corresponding to the equilibrium with the ultimate secondary product ($C_{\mathrm{min}}$). For example, if we consider the weathering of plagioclase under temperate conditions, the $C_{\mathrm{eq}}$ (here $C_{\mathrm{plag}}$) term represents the Si, Ca or Na ion concentration at equilibrium (at fixed temperature and pressure). The ultimate secondary product formed in the largest fractures in a temperate climate is kaolinite. Hence, the lowest concentration level ($C_{\mathrm{min}}$) is the concentration of ion species $i$ (Si, Ca or Na ions) at kaolinite equilibrium ($C_{\mathrm{kaol}}$). Consequently, the concentration range ($C_{\mathrm{eq}}-C_{\mathrm{min}}$) in the set of microsystems under consideration is given by ($C_{\mathrm{plag}}-C_{\mathrm{kaol}}$). In tropical regions or in high-gradient topographic environments where the ultimate product is gibbsite, the concentration range ($C_{\mathrm{eq}}-C_{\mathrm{min}}$) is given by ($C_{\mathrm{plag}}-C_{\mathrm{gibb}}$).

## QUANTITATIVE PETROGRAPHICAL APPROACH

### *Geometrical parameters of porosity: constrictivity and tortuosity*

It is well known that the saprock and saprolite zones (regolith) have a relatively large water storage capacity but low permeability, whereas the fissured bedrock has a small storage capacity but a relatively high permeability (Wright & Burgess, 1992). White & Brantley (2003) claimed that "For natural weathering, large increase in time continue to increase weathering intensities and further decrease permeabilities and reaction affinities, leading to further declines in natural weathering rates with time". The fact that porosity increases and permeability decreases with increasing weathering intensity implies that some geometrical parameters of the porosity network have changed, i.e. constrictivity and tortuosity. These parameters are taken into account through the 'apparent diffusion coefficient' in classical Ficks type equations:

$$J_i = -D_{\mathrm{a}(i)}\frac{d\mu_i}{dl} \tag{7}$$

The 'apparent diffusion coefficient' ($D_{\mathrm{a}(i)}$) of a solute in a weathered rock is not a constant parameter. It varies spatially within the rock and changes with time because of the progressive dissolution of the primary minerals. These variations are taken into account in the following equation:

$$D_{\mathrm{a}(i)} = \frac{D_{0(i)}G}{\Gamma} \tag{8}$$

where $D_{0(i)}$: diffusion coefficient in free water ($\mathrm{m^2\ s^{-1}}$); $G$: geometrical factor (adimensional; $G<1$); and $\Gamma$: retardation factor (adimensional; $\Gamma>1$).

The geometric factor ($G$) is considered to be dependent on the constrictivity ($\delta$) and tortuosity ($\tau$) according to:

$$G = \delta/\tau^2 \tag{9}$$

Both the constrictivity and tortuosity are empirically related to porosity ($\Phi$) by analogy with Archie's law (Archie, 1942) using the electrical conductivity of rocks:

$$G = \alpha\Phi^{\mathrm{m}} \tag{10}$$

The experimental values of the m and $\alpha$ constants are 1 and 2 for clayey materials (Archie, 1942) and 0.71 and 0.58 for crystalline rocks (Parkhomenko, 1967). The values of m for compacted clays and argillites are 2 and 1.95 respectively (Mammar *et al*., 2001; Revil *et al*., 2005). The retardation factor is determined according to the following relation:

$$\Gamma = 1 - \frac{GrK_{\mathrm{d}(i)}}{\Phi} \tag{11}$$

where $\rho$: dry rock density ($\mathrm{g\ cm^{-3}}$); $K_{\mathrm{d}(i)}$: sorption coefficient of chemical species ($i$) ($\mathrm{m^3\ kg^{-1}}$) and $\Phi$: effective rock porosity.

Some experimentally measured $K_{\mathrm{d}}$ values for cations diffusing through different crystalline rocks are presented in Table 2 (Byegård *et al*., 2001). The $K_{\mathrm{d}}$ may vary by several orders of magnitude depending on the chemical characteristics of the ion species.

According to equation 6, to calculate the flux of a chemical component ($i$) it is necessary to know its apparent diffusion coefficient ($D_{\mathrm{a}(i)}$) and the

chemical potential gradient ($d\mu_i/dl$). Due to its significance in nuclear waste safety, $D_{a(i)}$ has been determined experimentally for various elements diffusing into different rocks. It has been shown to decrease by one order of magnitude with alteration in a granodiorite: $4.3\pm3.7\times10^{-11}$ and $9.7\pm2.4\times10^{-12}$ $m^2$ $s^{-1}$ for fresh and altered samples, respectively (Sato, 1999).

### *The residence time of diffusing ions*

The duration of a weathering episode can be considered as the time needed for a hard rock to lose its microstructure by collapsing under gravity. As plagioclase is the most unstable mineral, granites tend to lose their mechanical resistance rapidly and abruptly when $Na_2O$ contents decrease by ~50% (Righi & Meunier, 1995). The question is, how much time is needed for the rock to lose this mass ($M_{dx}$)? In other words, how much time is needed for a given mineral species to dissolve to a certain point, whereby the dissolved components diffuse to the large fractures where they are more rapidly leached out by the flowing solutions? To calculate this time, the parameter needed is not the mineral dissolution rate but the rate at which the dissolved components diffuse through the connected porosity. This rate depends on the residence time of the dissolved components in their diffusion path (Neretnieks, 1980; Carrera *et al*., 1998). Because different microsystems are activated along individual diffusion paths, the calculation of the residence time must integrate all the processes at work inside these microsystems. In particular, several retardation effects during the transit of the dissolved components from their source to the large fractures must be taken into account: the formation of secondary mineral phases (transitory fixation of dissolved components) and the absorption on the inner and outer surfaces of secondary minerals (chemical exchange) are both of key significance.

From an ionic point of view, a weathered rock is a porous matrix where diffusion and surface interactions represent the main transportation processes. Diffusion is controlled by concentration gradients imposed by flows within fractures, whilst surface interactions consist of cation sorption and anionic exclusion phenomena. Hence matrix diffusion, which integrates pore diffusion and surface interactions, is the process that controls the residence time of the dissolved components. It has been investigated experimentally by diffusion of iodine or fluorescein in granites and shales (Hadermann & Heer, 1996). These components are often considered to be chemically inert, because they are neither fixed into the crystal lattices of clay minerals and oxyhydroxides nor strongly adsorbed on their surfaces. However, it is well known that iodine anionic exclusion modifies the accessible porosity pathways within a rock.

The residence time depends mainly on the trajectory of molecules and ions in the fluid filling the pores and the microfractures of the rock. In other words, the residence time depends on pore network geometry and the reactivity of grain surfaces. For most of the chemical components involved in the alteration processes such as Si, Al, $Fe^{3+}$ (among others), the residence time is increased by: (1) their incorporation into the crystal lattices of secondary phases, (2) their adsorption on the inner and outer surfaces of clay minerals (Ca, Na) or oxyhydroxides (metallic trace elements) and (3) their adsorption on exchangeable sites (K, Mg) (may also occur with (1)). For (1), the retardation effect is very high because, to be liberated back into the solution, the secondary phases previously formed must be dissolved. The residence time of these components depends on the duration of the secondary phases in the weathering profile. Components of the second category are more easily liberated in the solution than those which are incorporated in the crystal lattice because the secondary phases do not need to be destroyed to liberate them. These components are only exchanged via solid–fluid reactions. The chemical behaviour of the third ion category is more complex. However, they can be used as indicators of weathering intensity in specific cases (Mg for mafic or ultramafic rocks; Meunier, 2005).

In summary, any alteration process can be simplified to the variation of the chemical potential gradient *vs.* residence time (Fig. 9). The transfer of a given cation from its source (dissolving primary mineral) to the large passageways (diffusion to advection) can be retarded once or several times by incorporation or adsorption into secondary phases. This means that the best markers of the alteration rate would be the components or elements for which the retardation effects are as small as possible. In temperate climatic conditions, the inert components such as Al and Fe can be discounted, as well as the mobile ones such as Si, K or Mg ions which are commonly incorporated in secondary clay minerals. The best candidates would

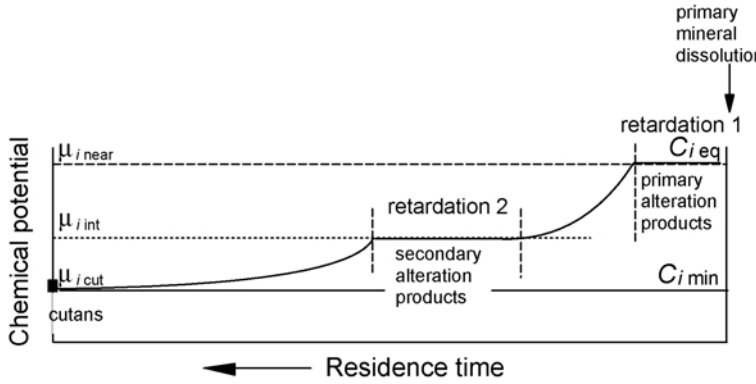


FIG. 9. Schematic representation of the relation between the residence time of a given dissolved element and its chemical potential in a weathered rock. The different retardation periods for that element are due to its temporary adsorption or incorporation in alteration products.

be Na and Ca, which are simply adsorbed as exchangeable cations in the interlayer zone of expandable clay minerals and also share similar $K_d$ values (Table 2). In tropical regions, where the accumulation levels in laterite profiles are dismantled, the markers should be Al and Fe ions, as in these areas the slowest process is no longer diffusion, but dissolution.

### *Calculating the residence time of a dissolved component in an altered rock*

A methodology based on the combination of quantitative petrography and laboratory diffusion experiments was developed to model the migration of solute toxic elements around nuclear waste storage. Here, the entire procedure (steps (i) to (vi), Table 3) was partially applied to different crystalline rocks: Palmottu granite, Kivetty and Grimsel granodiorites and Charroux-Civray granitic rocks (see references in Table 3). The Palmottu granite is the only example which was completely treated. Steps (v) and (vi) were investigated for non-interacting solutes ($\Gamma = 1$). The following steps were published separately (Table 3) and are brought together here to form a coherent analytical procedure:

(i) Petrography of the rock at different degrees of alteration (identification of the active microsystems). (ii) Quantitative petrography based on the image processing of porosity and mineral maps. The connected porosity is mapped after the sample is impregnated with $^{14}$C-PMMA. Mineral and porosity maps are also obtained from multi-element electron microprobe analysis (Prêt, 2003). (iii) Diffusion experiments: diffusion curves are obtained for the least reactive solute component in progressively altered rock samples (fresh–heavily

TABLE 2. Sorption coefficient ($K_d$) for different ionic species diffusing through the fine-grained Äspö granite and Äspö diorite (Byegård *et al*., 2001).

| Ionic species | $K_d$ ($m^3\ kg^{-1}$) Fine grained granite | $K_d$ ($m^3\ kg^{-1}$) Diorite |
|---|---|---|
| $Na^+$ | $^{\#}(4.5-8.2)\times10^{-6}$ | $^{\#}(0.3-1.3)\times10^{-6}$ |
| $Cs^+$ | $^{\#}470\times10^{-6}$ | $^{*}2500\times10^{-6}$ |
| $Sr^{2+}$ | $^{\#}(0.2-82)\times10^{-6}$ | $^{\#}(30-200)\times10^{-6}$ |
| $Ca^{2+}$ | $^{\#}(5.2-7.2)\times10^{-6}$ | $^{\#}(15-140)\times10^{-6}$ |
| $Ba^{2+}$ | $^{*}150\times10^{-6}$ | $^{\#}37\times10^{-6}$ |

$^{\#}$ $K_d$ evaluated from through-diffusion experiment results.
$^{*}$ $K_d$ evaluated from penetration experiments.

TABLE 3. The combined approach for calculating residence time distribution within the Palmottu granite (Finland). Details of the six steps are described in related papers.

| Step no. | Topic | Reference | Results |
|---|---|---|---|
| i | Classical Petrography | Siitari-Kauppi *et al*., 2003 | Mineralogical and petrophysical analysis |
| ii | Diffusion Experiment (lab) | Sardini *et al*., 2003 | Diffusion curve for non-interacting probe molecule |
| iii | Quantitative petrography | Oila *et al*., 2005 | Porosity distribution of primary mineral aggregates |
| iv | Diffusion Modelling | Sardini *et al*., 2003 | Validation of the Time Domain Diffusion method |
| v | Inverse Problem | Sardini *et al*., 2007 | Identification of two diffusion coefficients within rock matrix |
| vi | Residence Time Distribution | Robinet *et al*., in press | RTD for 'matrix diffusion' of solutes from a fracture |

altered) (Sardini *et al*., 2003). (iv) Diffusion simulations: the superimposed porosity and mineral maps are used as computation grids to condition diffusion pathways. Diffusion curves are calculated using the Time Domain Diffusion (TDD) procedure (Sardini *et al*., 2003). It should be noted that the local apparent diffusion coefficients remain unknown. (v) Inverse calculation of local diffusion parameters (Delay & Porel, 2003): the adjustment of local diffusion curves allows identification of the apparent diffusion coefficient ($D_a$) of each calculation cell. For Palmottu granite, it was found that the rock microstructure was characterized by two $D_a$ which are related to (1) microfissures and (2) the connected microporosity of altered plagioclase and biotite (Sardini *et al*., 2007). Tortuosity and constrictivity of diffusion paths within this connected porosity were found to be very high, emphasising the decrease of $D_a$ with increasing alteration rate. (vi) Calculation of residence times: previously determined values of $D_a$ are assigned to each cell of the calculation grids. For Palmottu granite, the residence time distribution was determined as defined by Carrera *et al*. (1998); it is the probability density function of the first passage times in the immobile domain (the rock matrix), given a Dirac pulse at the fracture surface (mobile domain). In this study it was obtained using a TDD method, with each particle initially located at the fracture/matrix interface (Robinet *et al*., 2007). The residence time of a particle refers to its return time within the fracture after transport within the matrix (Fig. 10a). The distribution is then obtained by iterative calculation from the return times of multiple particles. Even if this calculation does not correspond to the natural weathering condition, it provides the maximum diffusion times of chemically non-interacting particles in a granitic matrix, which was found to be >5000 y when considering a matrix thickness of only 4 cm. (vii) Calculation of the weathering duration: this is the final step of the process and has not yet been fully investigated. To complete the procedure, step (vi) has to be adapted to the weathering condition by imposing a source term for the entire rock matrix. Only then can the diffusion times from the rock matrix to the fracture be calculated (Fig. 10b).

## CONCLUSIONS

Weathering rate decreases with time in natural conditions because of two concomitant phenomena.

(1) The diffusion path length increases continuously as the dissolution of primary minerals progresses. This effect is enhanced by the increasing tortuosity and constrictivity of the connected porosity. Paradoxically, the altered rock becomes less permeable at the sample scale as porosity increases.

(2) The proportion of clay-coated surfaces in the connected porosity increases with time. The fluids which continuously invade the same passageways, are permanently in contact with the products of primary mineral alteration reactions. Namely, they are in contact with clays, oxyhydroxides and any remaining free primary mineral surfaces. As a result, even if granite weathering produces <10 wt.% clay minerals under temperate climatic

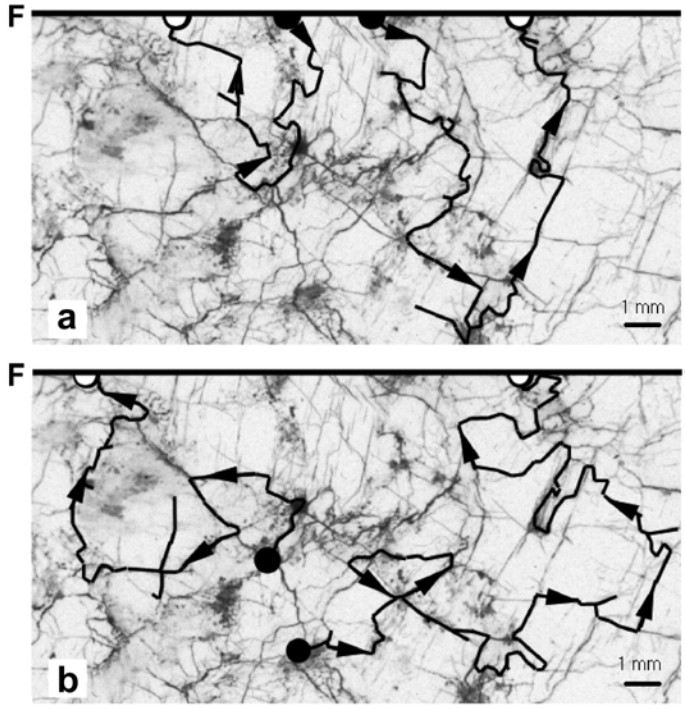


FIG. 10. Schematic representation of the particle-tracking method used for calculation of the residence time of a solute diffusing in a granite matrix from a fracture (F). The initial and final locations of each particle are represented by a black disk and an empty disk, respectively. For each case, two particle tracks are schematically represented. Case (a) represents a pollutant diffusing from a fracture surface and case (b) represents the weathering, where the initial location of the diffusing solute is distributed within the rock matrix.

conditions, the fluids which flow in the altered rock are essentially in contact with a clay-rich rock within the conduit system of the porosity. Consequently, the difference in chemical potential between the rock and fractures decreases with time. This effect is particularly intense in the zones where the rock structure has collapsed under gravity and formed new material (saprolite).

As weathering is a multi-scale phenomenon, theoretically any model needs to integrate the solid-fluid exchanges from the atomic interactions at the very surface of primary and secondary minerals (nanometre), to the rock sample (decimetre) and finally to the watershed (kilometre). However, such integration is currently beyond our calculation abilities. Hence we have to focus on the strategic aspect of weathering processes, although deciding where and on which variables to focus our attention remains difficult. It is remarkable that our understanding of the physicochemical weathering processes is much more advanced at the extreme scales of nanometres to tens/hundreds of kilometres, that at intermediate scales. At the nanometre level, the experimental and theoretical studies cover the observation of natural samples. The extensive use of high-resolution transmission electron microscopy (HRTEM), atomic force microscopy (AFM) and spectroscopy have significantly improved our knowledge of fluid-mineral reactions and their related interactions. Conversely, the large-scale studies based on isotope mass balance methods provide denudation rates for provinces or continents. Surprisingly, it is at the hand-specimen scale where efforts should now be directed.

## ACKNOWLEDGMENTS

This study was inspired from a book to be published (B. Velde & A. Meunier, *The Origin of Clay Minerals in Soils and Weathered Rocks*, Springer). This work is supported by UMR 6532 CNRS HYDRASA.

## REFERENCES


Allègre C.J., Dupré B., Négrel P. & Gaillardet J. (1986) Sr-Nd-Pb isotope systematics in Amazon and Congo river systems: constraints about erosion processes. *Chemical Geology*, **131**, 93–112.

Archie G.E. (1942) The electrical resistivity Log as an aid in determining some reservoir characteristics. *American Institute of Mineral and Metallurgical Engineering*, **1422**, 1–8.

Banfield J.F. & Barker W.W. (1994) Direct observation of reactant-product interfaces formed in natural weathering of exsolved, defective amphibole to smectite: evidence for episodic, isovolumetric reactions involving structural inheritance. *Geochimica et Cosmochimica Acta*, **58**, 1419–1429.

Banfield J.F. & Eggleton R.A. (1988) Transmission electron microscope study of biotite weathering. *Clays and Clay Minerals*, **36**, 47–60.

Banfield J.F. & Eggleton R.A. (1990) Analytical transmission electron microscope study of plagioclase, muscovite and K-feldspar weathering. *Clays and Clay Minerals*, **38**, 77–89.

Berner R.A. (1978) Rate control of mineral dissolution under Earth surface conditions. *American Journal of Science*, **278**, 1235–1252.

Berner R.A. (1981) Kinetics of weathering and diagenesis. Pp. 111–134 in: *Kinetics of Geochemical Processes* (A.C. Lasaga & R.J. Kirkpatrick, editors). Reviews in Mineralogy, **8**, Mineralogical Society of America.

Berner R.A. & Schott J. (1982) Mechanism of pyroxene and amphibole weathering – II. Observation of soil grains. *American Journal of Science*, **282**, 1214–1231.

Bisdom E.B.A. (1967) Micromorphology of a weathered granite near Ria de Arosa (NW Spain). *Leidse Geologische Mededelingen*, **37**, 33–67.

Brantley S.L. (2005) Reaction kinetics of primary rock-forming minerals under ambient conditions. Pp. 73–117 in: *Surface and Ground Water, Weathering and Soils* (J.J. Drever, editor) Treatise on Geochemistry, **5**, Elsevier, Amsterdam.

Brantley S.L. & Melott N.P. (2000) Surface area and porosity of primary silicate minerals. *American Mineralogist*, **85**, 1767–1783.

Byegård J., Widestrand H., Skålberg M., Tullborg E.L. & Siitari Kauppi M. (2001) Complementary investigation of diffusivity, porosity and sorptivity of Feature A-site specific geologic material. *International Cooperation Report*, **ICR-01-04**, 51 pp.

Carrera J., Sánchez-Vila X., Benet I., Medina A., Galarza G. & Guimerà J. (1998) On matrix diffusion: formulations, solution methods and qualitative effects. *Hydrogeology Journal*, **6**, 178–190.

Colman S.M. (1986) Levels of time information in weathering measurements, with examples from weathering rinds on volcanic clasts in the western United States. Pp. 379–393 in: *Rates of Chemical Weathering of Rocks and Minerals* (S.M. Colman & D.P. Dethier, editors). Academic Press Inc. Orlando, Florida, USA.

Delay F. & Porel G. (2003) Inverse modelling in the time domain for solving diffusion in a heterogeneous rock matrix. *Geophysical Research Lett*ers, **30**, 1147.

Dethier D.P. (1986) Weathering rates and chemical flux from catchments in the Pacific Northwest, U.S.A. Pp. 503–530 in: *Rates of Chemical Weathering of Rocks and Minerals* (S.M. Colman & D.P. Dethier, editors). Academic Press Inc. Orlando, Florida, USA.

Ebelmen M. (1847) Recherches sur la décomposition des roches. *Annales des Mines*, **12**, 627–654.

Eggleton R.A. (1984) Formation of iddingsite rims on olivine: a transmission electron microscope study. *Clays and Clay Minerals*, **32**, 1–11.

Eggleton R.A. & Buseck P.R. (1980) High resolution electron microscopy of feldspar weathering. *Clays and Clay Minerals*, **28**, 173–178.

Fontanaud A. & Meunier A. (1983) Mineralogical facies of a weathered serpentinized lherzolite from the Pyrénées, France. *Clay Minerals*, **18**, 77–88.

Gaillardet J., Dupré B., Louvat P. & Allègre C.J. (1999) Global silicate weathering and $CO_2$ consumption deduced from the chemistry of large rivers. *Chemical Geology*, **159**, 3–30.

Ganor J., Roueff E., Erel Y. & Blum J.D. (2005) The dissolution kinetics of a granite and its minerals – Implications for comparison between laboratory and field dissolution rates. *Geochimica et Cosmochimica Acta*, **69**, 607–621.

Garrels R.M. & Christ L.L. (1965) *Solutions, Minerals and Equilibria*. Freeman, Cooper, San Francisco, USA, 450 pp.

Gautier J.M., Oelkers E.H. & Scott J. (2001) Are quartz dissolution rates proportional to B.E.T. surface areas? *Geochimica et Cosmochimica Acta*, **65**, 1059–1070.

Hadermann J. & Heer W. (1996) The Grimsel (Switzerland) migration experiment: integrating field experiments, laboratory investigations and modelling. *Journal of Contaminant Hydrology*, **21**, 87–100.

Hellmuth K.H., Siitari-Kauppi M. & Lindberg A. (1993) Study of the porosity and migration pathways in crystalline rock by impregnation with $^{14}$C-polyméthylmethacrylate. *Journal of Contaminant Hydrology*, **13**, 403–418.

Hochella M.F. & Banfield J.F. (1995) Chemical weathering of silicates in nature: a microscopic perspective with theoretical considerations. Pp. 353–406 in: *Chemical Weathering Rates of Silicate Minerals* (A.F. White & S.L. Brantley, editors). Reviews in Mineralogy, **31**, Mineralogical Society of America.

Hodson M.E. (2003) The influence of Fe-rich coatings

on the dissolution of anorthite at pH 2.6. *Geochimica et Cosmochimica Acta*, **67**, 3355–3363.

Ildefonse P. (1980) Mineral facies developed by weathering of a meta-gabbro. Loire Atlantique (France). *Geoderma*, **24**, 257–273.

Korzhinskii D.S. (1959) *Physicochemical Basis of the Analysis of the Paragenesis of Minerals* (translation). Consultant Bureau, New York, 143 pp.

Mammar N., Rosanne M., Prunet-Foch B., Thovert J.F., Tevissen E. & Adler P.M. (2001) Transport properties of compact clays. 1. Conductivity and permeability. *Journal of Colloid and Interface Science*, **240**, 498–508.

Meunier A. (1980) Les mécanismes de l'altération des granites et le rôle des microsystèmes. Etude des arènes du massif granitique de Parthenay. *Mémoires de la Société Géologique de France*, **140**, 80.

Meunier A. (2005) *Clays*. Springer-Verlag, Berlin, 472 pp.

Meunier A. (2006) Why are clay minerals small? *Clay Minerals*, **41**, 551–566.

Meunier A. & Velde B. (1979) Weathering mineral facies in altered granites: the importance of local small-scale equilibria. *Mineralogical Magazine*, **43**, 261–268.

Millot G. (1964) *Géologie des Argiles*. Masson and C$^{ie}$, Paris, 499 pp.

Neretnieks I. (1980) Diffusion in the rock matrix: an important factor in radionuclide retardation. *Journal of Geophysical Research*, **85**, B8, 4379–4397.

Nugent M.A., Brantley S.L., Pantano S.G. & Maurice P.A. (1998) The influence of natural mineral coatings on feldspar weathering. *Nature*, **396**, 588–591.

Oila E., Sardini P., Siitari-Kauppi M. & Hellmuth K.H. (2005) The $^{14}$C-polymethylmethacrylate (PMMA) impregnation method and image analysis as a tool for porosity characterization of rock-forming minerals. Pp. 335–342 in: *Petrophysical Properties of Crystalline Rocks* (P.K. Harvey, T.S. Bewer, P.A. Pezard & V.A. Petrov, editors). Special Publication **240.** Geological Society, London**.**

Ollier C. & Pain C. (1996) *Regolith, Soils and Landforms*. John Wiley & Sons, Chichester, UK, 316 pp.

Pacheco F.A.L. & Alencoão A.M.P. (2006) Role of fractures in weathering of solid rocks: narrowing the gap between laboratory and field weathering rates. *Journal of Hydrology*, **316**, 248–265.

Parkhomenko E.I. (1967) *Electrical Properties of Rocks*, (translation G. V. Keller). Plenum Press, New York, 314 pp.

Prêt D. (2003) *Nouvelles méthodes quantitatives de cartographie de la porosité et de la minéralogie dans les matériaux argileux: application aux bentonites compactées des barrières ouvragées*. PhD thesis, Université de Poitiers, France, 240 pp.

Putnis A. (2002) Mineral replacement reactions: from macroscopic observations to microscopic mechanisms. *Mineralogical Magazine*, **66**, 689–708.

Revil A. (1999) Ionic diffusivity, electrical conductivity, membrane and thermoelectric potentials in colloids and granular porous media: a unified model. *Journal of Colloid Interface Science*, **212**, 503–522.

Revil A., Leroy P. & Titov K. (2005) Characterization of transport properties of argillaceous sediments: application to the Callovo-Oxfordian argillite. *Journal of Geophysical Research*, **110**, 1–18.

Righi D. & Meunier A. (1995) Origin of clays by rock weathering and soil formation. Pp. 43–161 in: *Origin and Mineralogy of Clays: Clays and the Environment* (B. Velde, editor), Springer-Verlag, Heidelberg, Germany.

Robinet J.C., Sardini P., Delay F. & Hellmuth K.H. (2007) The effect of rock matrix heterogeneities near fracture walls on the residence time distribution (RTD) of solutes. *Transport in Porous Media* (in press).

Sak P.B., Fisher D.M., Gardner T.W., Murphy K. & Brantley S.L. (2004) Rates of weathering rind formation on Costa Rican basalt. *Geochimica et Cosmochimica Acta*, **68**, 1453–1472.

Sardini P., Sammartino S. & Tévissen E. (2001) An image analysis contribution to the study of transport properties of low-permeability crystalline rocks. *Computer Geosciences*, **27**, 1051–1059.

Sardini P., Delay F., Hellmuth K.H., Porel G. & Oila E. (2003) Interpretation of diffusion experiments on crystalline rocks using random walk modelling. *Journal of Contaminant Hydrology*, **61**, 339–350.

Sardini P., Siitari-Kaupi M., Beaufort D. & Hellmuth K.H. (2006) On the connected porosity of mineral aggregates in crystalline rocks. *American Mineralogist*, **91**, 1069–1080.

Sardini P., Robinet J.C., Siitari-Kauppi M., Delay F. & Hellmuth K.H. (2007) Direct simulation of heterogeneous diffusion and inversion procedure applied to an out-diffusion experiment. Test case of Palmottu granite. *Journal of Contaminant Hydrology*, **93**, 21–37.

Sato H. (1999) Matrix diffusion of some simple cations, anions, and neutral species in fractured crystalline rocks. *Nuclear Technology*, **127**, 199–211.

Sausse J., Jacquot E., Leroy J. & Lespinasse M. (2001) Evolution of crack permeability during fluid-rock interaction. Example of the Brézouard granite (Vosges, France). *Tectonophysics*, **336**, 199–214.

Siitari-Kauppi M., Marcos N., Klobes P., Goebbels J., Timonen J. & Hellmuth K.H. (2003) The Palmottu natural project. Physical rock matrix characterisation. *Geological Survey of Finland Report*, **YST118**, 63 pp.

Tardy Y. (1993) *Pétrologie des Latérites et des Sols tropicaux*. Masson, Paris, 535 pp.

Velbel M.A. (1993) Formation of protective surface

layers during silicate-mineral weathering under well-leached, oxidizing conditions. *American Mineralogist*, **78**, 405–414.

White A.F. & Brantley S.L. (1995) Chemical weathering rates of silicate minerals: an overview. Pp. 1–22 in: *Chemical Weathering Rates of Silicate Minerals* (A.F. White & S.L. Brantley, editors). Reviews in Mineralogy, **31**, Mineralogical Society of America, Washington, D.C.

White A.F. & Brantley S.L. (2003) The effects of time on the weathering of silicate minerals: why do weathering rates differ in the laboratory and field? *Chemical Geology*, **202**, 479–506.

White A.F., Bullen T.D., Schulz M.S., Blum A.E., Huntington T.G. & Peters N.E. (2001) Differential rates of feldspar weathering in granitic regoliths. *Geochimica et Cosmochimica Acta*, **65**, 847–869.

Whitehouse I.E., McSaveney M.J., Knuepfer P.L.K. & Chinn T.J.H. (1986) Growth of the weathering rinds on Torlesse Sandstone, Southern Alps, New Zealand. Pp. 419–435 in: *Rates of Chemical Weathering of Rocks and Minerals* (S.M. Colman & D.P. Dethier, editors). Academic Press Inc., Orlando, Florida, USA.

Wilson M.J. (2004) Weathering of the primary rock-forming minerals: processes, products and rates. *Clay Minerals*, **39**, 233–266.

Wright E.P. & Burgess W.D. (1992) *The Hydrology of Crystalline Basement Aquifers in Africa*. Special Publication **66**. Geological Society, London. 264 pp.